Supplementary materials

S1. Distribution of social network ego-betweenness centrality score

The following is the distribution of the ego-betweenness centrality score of the participants. The median score is 0.7.

Figure S1. Distribution of ego-betweenness centrality score

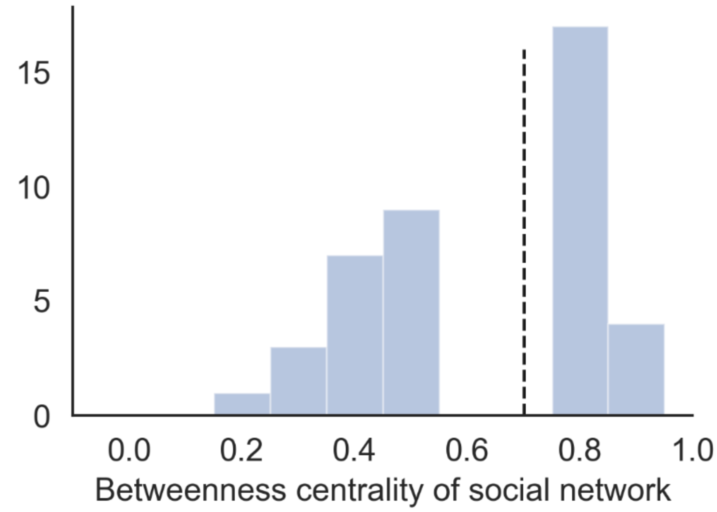

S2. Peak coordinates of whole-brain maps showing significant encoding consistency

Below is the list of peak coordinates (Table S1) where significant encoding consistency was found under each condition (c.f. Figure 4).

Table S1. Peak MNI coordinates of clusters (k > 30) with significant encoding consistency

	L/R	**x**	**y**	**z**	***t***	**k**
Read						
Lingual	R	12	-55	7	9.88	18072
Occipital Mid	L	-48	-73	1	5.53	56
Precentral	R	21	-16	73	4.17	33
Broadcast						
Calcarine	R	9	-85	-2	8.00	8965
Temporal Pole Mid	R	39	11	-35	7.59	1719
Parietal Inf	R	54	-46	55	5.57	221
Paracentral Lobule	R	12	-31	49	4.38	154
Rectus	R	6	62	-17	5.37	101
Cerebellum	R	27	20	4	4.84	66
Thalamus	R	6	-19	4	4.46	58
Temporal Sup	R	45	-37	16	6.29	55
Frontal Inf Tri	R	30	14	28	5.04	49
Calcarine	R	27	-67	13	5.67	38
Cingulate Ant	L	-9	29	19	3.85	36
Cerebellum	R	27	-52	-47	4.60	33
Narrowcast						
Calcarine	R	21	-67	16	7.51	3898
Temporal Mid	L	-51	-43	10	7.04	1400
Frontal Inf Tri	R	51	23	-2	7.32	1177
Frontal Med Orb	R	6	62	-11	6.14	748
Frontal Sup	L	-24	2	52	6.15	408
Cingulate Mid	R	15	20	37	5.61	273
Frontal Sup	R	21	20	40	5.34	118
Cingulate Ant	R	12	41	16	4.36	93
Cerebellum	L	-36	-61	-38	5.92	92
Parietal Sup	L	-18	-64	67	4.22	73
Cerebellum	L	-21	-91	-29	4.58	66
Precentral	R	60	-10	49	4.97	61
Precentral	R	33	-10	55	5.35	61
Parietal Sup	R	21	-61	67	4.14	52
Amygdala	L	-27	5	-17	5.16	48
Parietal Inf	L	-54	-34	37	4.55	37
Parietal Inf	R	51	-43	52	4.47	32
Putamen	R	30	14	7	3.68	32
Angular	R	39	-61	34	4.31	31

S3. Whole-brain analysis of encoding consistency in the content condition

Although the content condition was not our focal interest of this study, we conducted similar analyses with that condition. We found similar encoding consistency effect in sensory cortices, temporal lobe and higher-order regions (Figure S2A).

When we compared all other conditions to the content condition (which focused on content comprehension instead of evaluation; Figure S2B), we found the read condition had stronger encoding consistency in PCC (peak at [6 -58 7], 377 voxels), bilateral angular gyrus (R: [42 -70 46], 160 voxels; L: [-36 -67 34], 124 voxels) and vmPFC ([12 41 -17], 101 voxels). On the other hand, we found stronger encoding consistency for the content condition at left inferior frontal gyrus ([-51 35 -2], 81 voxels), an area involved in semantic processing.

Compared to narrowcast condition, the content condition had stronger encoding consistency at MPFC ([-30 50 28], 48 voxels) and left inferior frontal gyrus ([-54 14 22], 28 voxels). The broadcast condition had stronger consistency in cerebellum ([-27 -82 -38], 56 voxels; [-12 -67 -26], 45 voxels).

Figure S2. Whole-brain comparison of encoding consistency between narrowcast and broadcast conditions ($p < .05$ FDR adjusted)

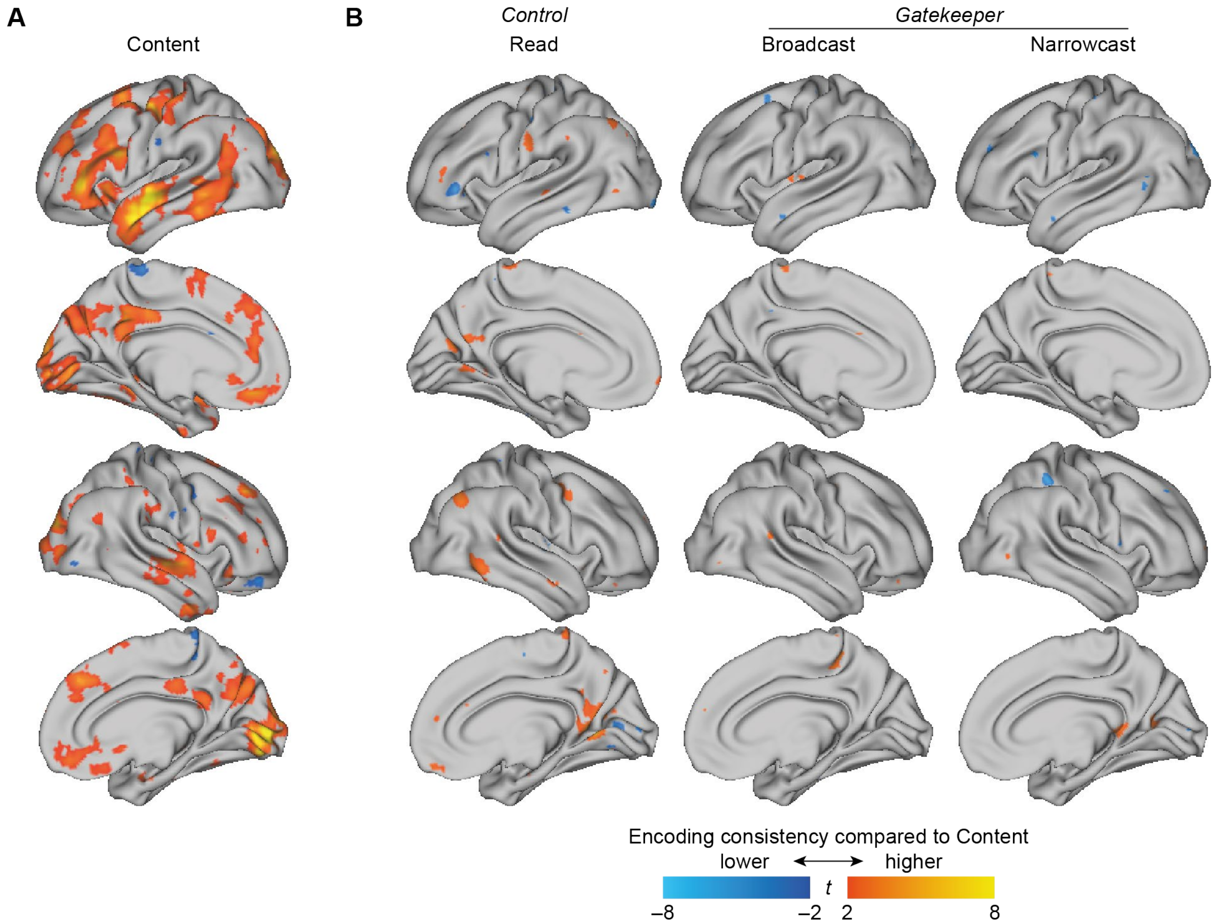

S4. Whole-brain comparison of encoding consistency between narrowcast and broadcast conditions

We conducted the whole-brain comparison of encoding consistency between the two sharing conditions (narrowcast and broadcast) (Figure S3 and Table S2).

Figure S3. Whole-brain comparison of encoding consistency between narrowcast and broadcast conditions ($p < .05$ FDR adjusted)

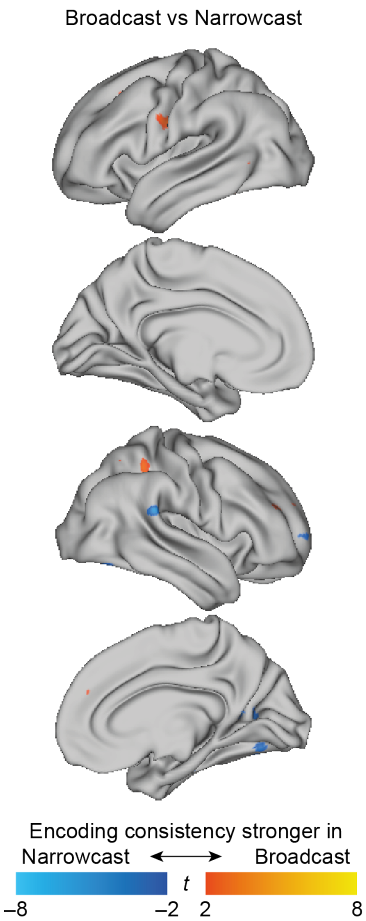

Table S2. Peak MNI coordinates of clusters (k > 30) with significant difference in encoding consistency between narrowcast and broadcast conditions

	L/R	x	y	z	*t*	k
Broadcast > Narrowcast						
Middle frontal gyrus	L	-45	44	22	6.05	46
Precentral gyrus	L	-48	-7	28	5.95	40
Narrowcast > Broadcast						
Posterior cingulate cortex	R	12	-55	13	-6.19	60
Fusiform cortex	R	30	-67	-11	-5.77	36

S5. Whole-brain activation under the sharing conditions

In addition to pattern analysis, we conducted a GLM analysis comparing activations across different conditions (Figure S4). At the first level, the four conditions (content, read, narrowcast and broadcast) were entered as regressors, together with six motion regressors and average grand and white matter signals. Second level contrasts were computed between read and narrowcast, and between read and broadcast. We found that the narrowcast condition (compared to the read condition) had stronger activation at precuneus, MPFC and angular gyri (but not fusiform gyri), indicating that participants recruited these regions when they evaluated whether to share the information with others. On the other hand, no significant clusters were found for the broadcast condition.

Figure S4. Whole-brain comparison of activation under sharing conditions ($p < .05$ FDR adjusted)

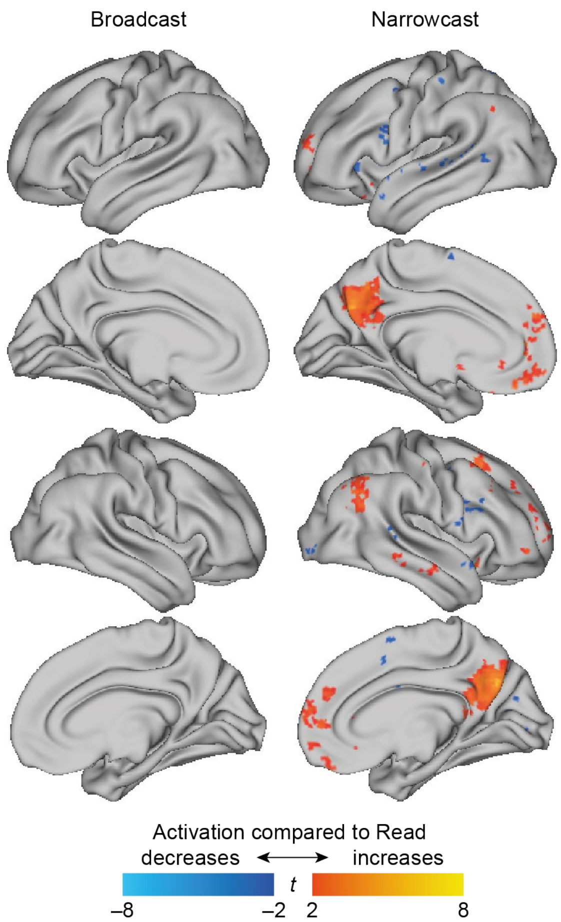

S6. Self-reported ratings and ego-betweenness centrality

Did a participant's ego-betweenness centrality score affect the variability of their own self-report ratings (i.e., how much the participants liked to read for themselves, share with their friends, or share on their Facebook feed)?

We first examined the mean self-report rating difference (pairwise absolute difference in rating [1-5] across participants on the same article within the same condition). We found that on average, participants had more diverse ratings on reading intention compared to sharing conditions (greater average mean absolute difference). In particular, ratings were most similar in the narrowcast condition (Figure S5A).

Next, we examined whether ego-betweenness centrality was associated with the rating difference among participants, by comparing ego-betweenness centrality matrices and rating difference matrices. We found a negative correlation in the narrowcast condition, meaning that participants with high ego-betweenness centrality tended to agree more (i.e., be less dissimilar) on the intention to share with friends (Figure S5B).

Figure S5. (A) Mean rating difference of participants across conditions. Comparisons are made based on same-article paired non-parametric Wilcoxon test. (B) Mean correlation (denoted in black squares) between neural-based dissimilarity matrix and rating difference matrix under each condition. Shaded areas are violin plots of the null distributions of 10,000 permutations.

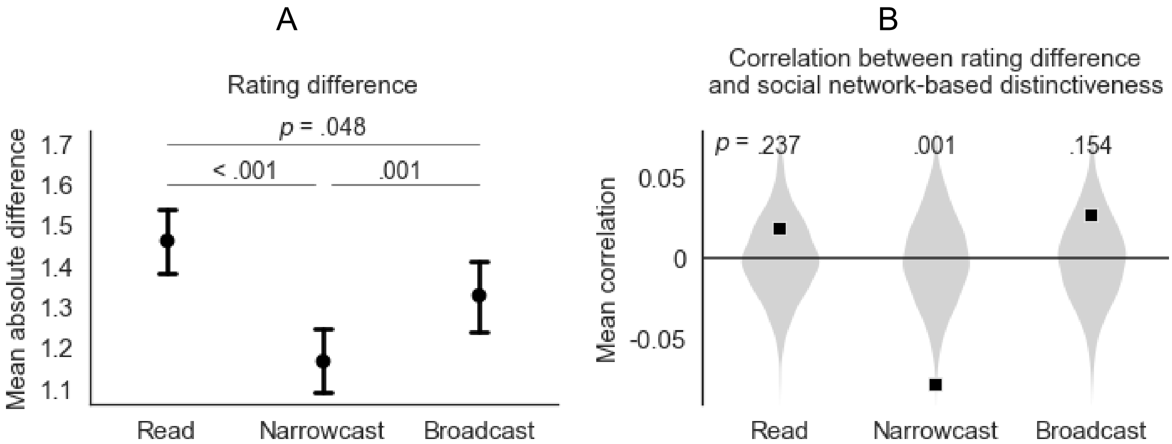

S7. Self-reported ratings and differential neural encoding

We investigated whether self-reported ratings of the articles (how much the participants liked to read for themselves, share with their friends, or share on their Facebook feed) were also associated with differential neural encoding. By comparing the neural dissimilarity matrix and the rating difference matrix, we found a positive correlation in the read condition, meaning that participants who rated similar reading preferences had more similar neural patterns within the key regions of interest in MPFC, precuneus and other regions defined in Figure 4 of the main manuscript.

Figure S6. Mean correlation (denoted in black squares) between neural-based dissimilarity matrix and rating difference matrix under each condition. Shaded areas are violin plots of the null distributions of 10,000 permutations.